PHYSICAL REVIEW A **79**, 010702(R) (2009)

Quantum theory of ultracold atom-ion collisions

Zbigniew Idziaszek,[1] Tommaso Calarco,[2,3] Paul S. Julienne,[4] and Andrea Simoni[5]
[1]*Institute of Theoretical Physics, University of Warsaw, 00-681 Warsaw, Poland*
[2]*Institute of Quantum Information Processing, University of Ulm, D-89069 Ulm, Germany*
[3]*European Centre for Theoretical Studies in Nuclear Physics and Related Areas, I-38050 Villazzano (TN), Italy*
[4]*Joint Quantum Institute, NIST and the University of Maryland, Gaithersburg, Maryland 20899-8423, USA*
[5]*Institut de Physique de Rennes 1, UMR 6251 du CNRS and Université de Rennes, 35042 Rennes Cedex, France*
(Received 25 June 2008; published 15 January 2009)

We study atom-ion scattering in the ultracold regime. To this aim, an analytical model based on the multichannel quantum-defect formalism is developed and compared to close-coupled numerical calculations. We investigate the occurrence of magnetic Feshbach resonances, focusing on the specific $^{40}Ca^{+}+Na$ system. The presence of several resonances at experimentally accessible magnetic fields should allow the atom-ion interaction to be precisely tuned. A fully quantum-mechanical study of charge-exchange processes shows that charge-exchange rates should remain small even in the presence of resonance effects. Most of our results can be cast in a system-independent form and are important for the realization of charge-neutral ultracold systems.

DOI: 10.1103/PhysRevA.79.010702 PACS number(s): 34.50.Cx, 34.70.+e, 34.90.+q

Advances in trapping, cooling, manipulation, and readout of single atoms and ions have led over recent years to a range of fundamental as well as applied investigations on the quantum properties of such systems. Nowadays, an increasing number of experimental groups worldwide are starting experiments with combined charged-neutral systems in various configurations [1]. While the theory of atom-ion collisions is well established for high collision energies [2,3], a theoretical description in the ultracold domain is still largely missing.

This Rapid Communication presents a study of magnetic Feshbach resonances and a fully quantum study of the radiative charge exchange process for ultracold atom-ion systems that includes effects of Feshbach and shape resonances. Here we consider only two-body collisions in free space, a necessary prelude to further studies incorporating effects of ion micromotion or trap confinement. We develop a reliable yet manageable effective model of atom-ion collisions by applying multichannel quantum defect theory (MQDT) [4–6] based on the long-range ion-induced-dipole potential that varies as r^{-4} at large ion-atom distance r [7,8]. This powerful tool has proven effective as a few-parameter approach for describing scattering and bound states in electron-ion core [4], electron-atom [9], and neutral-atom systems [10]. Although literature on the subject is rich, here we discuss some details of MQDT illustrating how it works in the ultracold domain, so we can reveal the new and interesting ultracold ion-atom physics. We adapt MQDT to the atom-ion realm, utilizing the analytical solutions for the r^{-4} asymptotic potential [9,11] and applying the frame transformation [10,12] at short distances to reduce the number of quantum defect parameters in the model. We verify the model predictions by comparing to our own numerical close-coupled calculations, taking $^{40}Ca^{+}-^{23}Na$ [13] as a reference system.

We describe the *S*-state atom and *S*-state ion collisions with the close-coupled radial Schrödinger equation

$$\frac{\partial^2 \mathbf{F}}{\partial r^2} + \frac{2\mu}{\hbar^2}[E - \mathbf{W}(r)]\mathbf{F}(r) = 0. \tag{1}$$

Here, $\mu = m_i m_a/(m_i+m_a)$ denotes the reduced mass, $\mathbf{W}(r)$ is the interaction matrix, and $\mathbf{F}(r)$ is the matrix of radial solutions. The wave function for N scattering channels reads $\Psi_i(\mathbf{r}) = \Sigma_{j=1}^{N} A_j Y_j(\hat{\mathbf{r}}) F_{ij}(r)/r$, where $Y_j(\hat{\mathbf{r}})$ denotes the angular part of the solution for the scattering channel j and the constant vector $\mathbf{A}$ is determined by the boundary conditions at $r \to \infty$. The asymptotic channel states can be characterized by the hyperfine quantum numbers f_1, m_{f_1} and f_2, m_{f_2} for ion and atom, respectively, and by the angular momentum quantum numbers l and m_l of the relative motion of the atom and ion centers of mass. We denote the asymptotic channel states by $|\Psi_\alpha\rangle$, where $\alpha = \{f_1 f_2 m_{f_1} m_{f_2} l m_l\}$. In the presence of a magnetic field B, the field-dressed channel states $|\Psi_\alpha(B)\rangle$ are linear combinations of the bare $(B=0)$ channel states $|\Psi_\alpha(B)\rangle = \Sigma_{\alpha'} Z_{\alpha\alpha'}(B)|\Psi_{\alpha'}\rangle$. In the asymptotic channel basis the interaction matrix is diagonal at large distances:

$$W_{ij}(r) \overset{r\to\infty}{\sim} \left[E_i^{\infty} + \frac{\hbar^2 l(l+1)}{2\mu r^2} - \frac{C_4}{r^4}\right]\delta_{ij} + O(r^{-6}), \tag{2}$$

where E_i^{∞} are the threshold energies for the channel i including the hyperfine energies and Zeeman shifts, and $C_4 = \alpha e^2/2$, with α denoting the static dipolar polarizability of the atom and e is the ion charge. At typical distances R_0 where the short-range exchange interaction takes place, the interaction matrix becomes diagonal in the *IS* representation, characterized by total electron spin $\mathbf{S} = \mathbf{s}_1 + \mathbf{s}_2$, total nuclear spin $\mathbf{I} = \mathbf{i}_1 + \mathbf{i}_2$, total hyperfine angular momentum $\mathbf{F} = \mathbf{f}_1 + \mathbf{f}_2 = \mathbf{I} + \mathbf{S}$, and its projection M_F on the axis of quantization, where $\mathbf{s}_1$ and $\mathbf{s}_2$ are the electron spin of ion and atom, respectively, and $\mathbf{i}_1$ and $\mathbf{i}_2$ denote their nuclear spins, respectively. We label those channels by $\beta = \{ISFM_F l m_l\}$.

With the long-range atom-ion one can associate the length scale $R^* \equiv \sqrt{2C_4\mu/\hbar^2}$ and energy scale $E^* = \hbar^2/[2\mu(R^*)^2]$. The length R^* can be also related to the position of the last node of the zero-energy *s*-wave radial wave function for the

scattering length $a=0$: $L=(2/\pi)R^*$. The maxima due to the centrifugal barrier occur at $r_{\max}=(\sqrt{2}/\sqrt{l(l+1)})R^*$ and have heights of $E_{\max}=\frac{1}{4}l^2(l+1)^2E^*$. Hence E^* determines the contribution of higher partial waves in the atom-ion scattering.

The basic idea of MQDT [4–6] is the separation between the short-range and long-range properties of the scattering wave function. The short-range wave function is insensitive to the total energy E and, in the case of atom-ion collisions, also to the relative orbital angular momentum [14]. On the contrary, at large distances the wave function varies rapidly with E, as well as other scattering quantities defined at $r\to\infty$. By introducing a set of short-range quantum-defect parameters, MQDT allows one to determine all scattering and bound-state properties in a wide range of collision energies.

In MQDT one starts by choosing a set of reference potentials $\{V_j(r)\}$, which reproduce the asymptotic behavior of the interaction matrix at large distances: $V_j(r)\sim W_{jj}(r)$ $(r\to\infty)$, but otherwise can be arbitrary. With the reference potentials $V_i(r)$ one can associate a pair of linearly independent solutions $\hat{f}_i(r)$ and $\hat{g}_i(r)$:

$$\hat{f}_i(r)=\alpha_i(r)\sin\beta_i(r), \tag{3}$$

$$\hat{g}_i(r)=\alpha_i(r)\cos\beta_i(r). \tag{4}$$

The amplitude $\alpha_i(r)$ fulfills the inhomogeneous Milne equation $[d^2/dr^2+k_i(r)^2]\alpha(r)=\alpha^{-3}(r)$ [15], with the local wave vector $k_i(r)=\sqrt{2\mu[E-V_i(R)]}/\hbar$, while the phase $d\beta_i/dr=1/\alpha_i^2$. We impose WKB-like boundary conditions at small distances, $\alpha_i(r)\cong 1/\sqrt{k_i(r)}$ and $\alpha_i'(r)\cong 0$, which makes the functions $\hat{f}_i(r)$ and $\hat{g}_i(r)$ weakly dependent on energy. The exact solution to Eq. (1) at large distances [where $V_j(r)\cong W_{jj}(r)$] can be expressed in terms of $\hat{f}_i(r)$ and $\hat{g}_i(r)$: $\mathbf{F}(r)\sim[\hat{\mathbf{f}}(r)+\hat{\mathbf{g}}(r)\mathbf{Y}(E)]\hat{\mathbf{A}}$ $(r\to\infty)$. Here, $\hat{\mathbf{f}}(r)\equiv\mathrm{diag}[\hat{f}_i(r)]$, $\hat{\mathbf{g}}(r)\equiv\mathrm{diag}[\hat{g}_i(r)]$, and $\mathbf{Y}(E)$ is the energy-insensitive $[\mathbf{Y}(E)\cong\mathbf{Y}]$ quantum-defect matrix that plays a central role in the quantum-defect analysis.

The Schrödinger equation with the polarization potential C_4/r^4 can be solved analytically in terms of Mathieu functions of imaginary argument [11,16]. For our choice of MQDT reference potentials, $V_i(r)=C_4/r^4+l(l+1)/r^2+E_i^\infty$, the solutions $\hat{f}$ and $\hat{g}$ are singular at $r\to 0$ [17]:

$$\hat{f}(r)\cong r\sin(-R^*/r+\varphi)\quad(r\to 0), \tag{5}$$

$$\hat{g}(r)\cong r\cos(-R^*/r+\varphi)\quad(r\to 0). \tag{6}$$

Here, φ denotes some short-range phase that can be related to the s-wave scattering length $a=-R^*\cot\varphi$ of the C_4/r^4 potential [17]. In view of the arbitrariness of the reference potential, we set $\varphi=0$, which does not affect the physical scattering matrices, which are not sensitive to the short-range behavior of the reference potentials.

The frame transformation (FT) is a unitary transformation between channels α and β, $U_{\alpha\beta}=(f_1f_2m_{f_1}m_{f_2}|ISFM_F)$, which can be expressed in terms of the usual Clebsch-Gordan and Wigner $9j$ symbols (see, e.g., [10]). The application of FT requires $R_0\ll R^*$, which is typically very well fulfilled in the atom-ion collisions. At distances $r\gtrsim R_0$ the exchange interaction is no longer present, and for $r\ll R^*$ we can safely neglect both the centrifugal potential and hyperfine splittings and also ignore the higher-order dispersion terms C_6/r^6 and C_8/r^8, which lead only to small corrections (see below). Then for $R_0\lesssim r\ll R^*$, $W_{ij}(r)\cong\delta_{ij}C_4/r^4$, and the wave function in each of the channel is simply given by the linear combination of the two short-range solutions (5) and (6), both in the asymptotic and (*IS*) representations.

In view of the assumed form of the reference potentials and the choice $\varphi=0$, the quantum-defect matrix in *IS* representation takes the form $Y^{(IS)}_{\beta\beta'}=\delta_{\beta\beta'}[a_{S(\beta)}]^{-1}$, where $S(\beta)$ is the total electron spin in the channel β, which takes values $S(\beta)=0,1$ corresponding to the singlet a_s and triplet a_t scattering lengths, respectively. Then, $\mathbf{Y}$ in the basis of the asymptotic channel states reads $\mathbf{Y}=\mathbf{Z}(B)\mathbf{U}\mathbf{Y}^{(IS)}\mathbf{U}^\dagger\mathbf{Z}^\dagger(B)$, where $\mathbf{Z}(B)$ is the transformation from bare to the magnetic-field-dressed states. Finally, the $\mathbf{S}$ and $\mathbf{K}$ matrices describing all the scattering properties, including the cross sections, are calculated directly from $\mathbf{Y}$ with the help of the quantum-defect functions [5,6], which are determined by the asymptotic behavior of the short-range normalized solutions $\hat{f},\hat{g}$.

We now apply our model to a system of $^{40}Ca^+$ and ^{23}Na for which the long-range parameter $C_4=81.35$ a.u. and the short-range *ab initio* potential curves are approximately known [13]. The close-coupled Schrödinger equation (1) is solved both within our MQDT approach and exactly using standard numerical methods.

Unfortunately, potentials calculated by *ab initio* methods are usually not sufficiently accurate to predict the value of the associated scattering lengths. Therefore, for our calculation we will either assume typical magnitudes of a_s and a_t on the order of R^* or we vary them. It is interesting to note that for a r^{-4} potential the probabilities to find a positive or a negative scattering length are equal in contrast to van der Waals r^{-6} interaction where their ratio is 3:4 [18].

The ^{40}Ca ion has vanishing nuclear spin ($i_1=0$), whereas the ^{23}Na atom has $i_2=3/2$, resulting in a total hyperfine angular momentum $f_2=1$ and $f_2=2$. Neglecting small anisotropic spin interactions, rotational invariance implies that l, m_l, and M_F are conserved quantities. In our calculations we will consider collisions in the $M_F=1/2$ block and use the FT to obtain $\mathbf{Y}$ in the asymptotic channel representation. At $B=0$ the off-diagonal elements of $\mathbf{Y}$ are proportional to $1/a_c=1/a_s-1/a_t$, where a_c is an effective scattering length characterizing the strength of channel coupling.

We begin our analysis by considering a single $A\,^1\Sigma^+$ potential as entrance channel. The upper panel of Fig. 1 shows the rate $v\sigma_l$ of elastic Ca^++Na collisions as a function a collisions energy for different partial waves, with v the relative atomic velocity and σ_l the partial wave cross section. The calculation is performed using a potential parametrized by a scattering length of $a_s=-0.961R^*=-2000a_0$. One can observe several dips of the collisional rates, corresponding to Ramsauer minima. We note that because of the relatively low centrifugal barriers, partial waves with $l>0$ give a significant contribution already in the μK regime. At small ener-

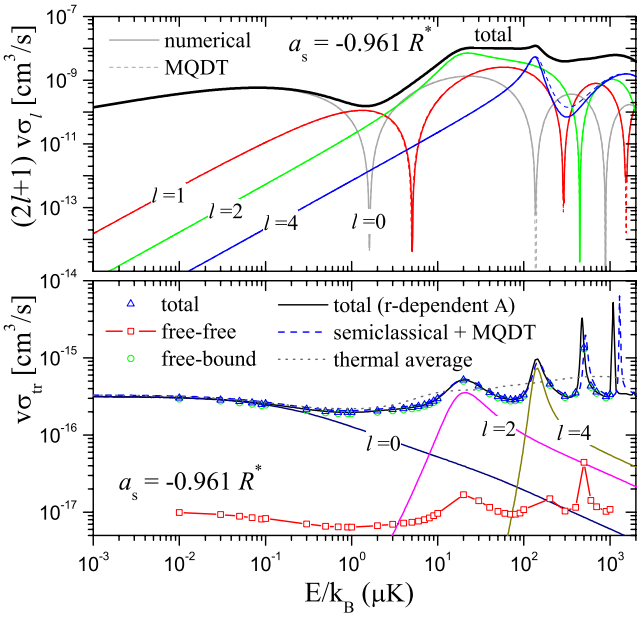

FIG. 1. (Color online) Elastic collision rate in the singlet channel $A\ ^1\Sigma^+$ (upper panel) and rate of radiative $A\ ^1\Sigma^+ \rightarrow X\ ^1\Sigma^+$ charge transfer (lower panel) versus collision energy. Different theoretical approaches are compared (see text). Both the elastic and total inelastic rates are decomposed on selected partial waves.

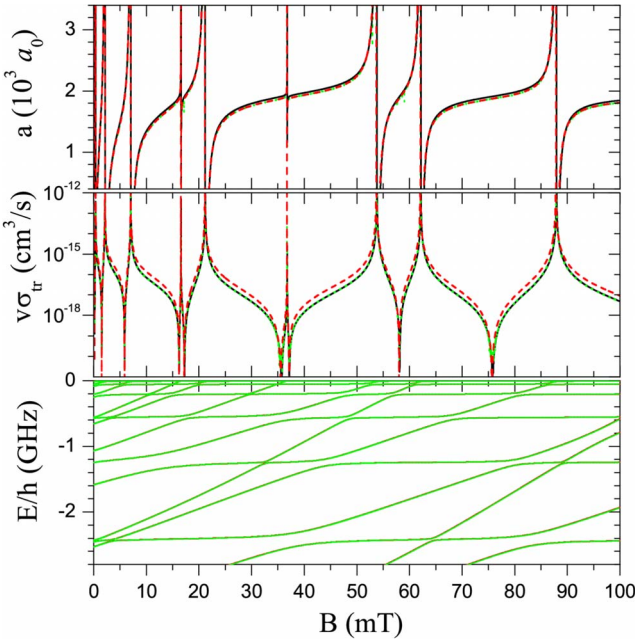

FIG. 2. (Color online) Field-dependent s-wave scattering length (upper panel), charge-transfer rate for s-wave collisions at $E=1$ nK (middle panel) and energies of $l=0$ bound states (lower panel) as a function of the magnetic field strength B, for $a_s=-0.9R^*$ and $a_t=-a_s$. Close-coupled numerical calculations with (solid line) and without higher-order dispersion terms (dotted line) and the MQDT results (dashed line) are compared. Results from different approaches are undistinguishable on the scale of the bottom panel.

gies the rates for $l>0$ behave asymptotically as $\sigma_l v \sim E^{3/2}$, in agreement with the threshold behavior typical of r^{-4} potentials [19]. For $l=4$ and at higher energies some discrepancies between the numerical and MQDT approaches can be observed, resulting from a breakdown of the assumption of angular momentum insensitivity of the quantum-defect matrix in the analytical model. On the basis of the MQDT model, one can argue that the elastic collisional rates in the triplet channels would be of similar order, with the particular structure of maxima and Ramsauer minima determined by the value of a_t.

The lower panel of Fig. 1 shows the total rate $v\sigma_{tr}$ of inelastic $A\ ^1\Sigma^+ \rightarrow X\ ^1\Sigma^+$ collisions associated with radiative charge transfer (see [13] for details). The numerical results (first three entries in the legend) have been obtained in the distorted-wave Born approximation by summing contributions from all free-free and free-bound transitions [20]. Note that molecular ions are formed with very high probability (~96%) in the electron-exchange process. The figure also shows the total charge-exchange rate obtained by a computationally much simpler single-channel calculation with a position-dependent Einstein coefficient $A(r)$ (see, e.g., [21]). In addition, we show the result of our analytical model where the charge-transfer probability has been described in the semiclassical theory, while MQDT provides a proper rescaling of the wave function between reaction and asymptotic zones. One can observe that the three numerical and analytical approaches give virtually the same result for the total (free-free plus free-bound) charge-exchange rate at low energy. It is only at higher energies, in particular near the peaks associated with shape resonances, that the MQDT model becomes less accurate. This can again result from the modification of the quantum-defect matrix Y for higher l.

In contrast to the purely semiclassical result of Ref. [13], both elastic and inelastic quantum cross sections appear to be strongly affected by the presence of shape resonances up to mK regime; see Fig. 1. We have verified that this is a general behavior not related to the particular choice of the singlet scattering length assumed for the calculation. The influence of shape resonances can also be observed in the thermally averaged rate, which only begins to saturate to the asymptotic value in the mK regime.

Next, we take into account multichannel hyperfine effects and the presence of an external magnetic field. Figure 2 shows the variation of the effective scattering length a versus magnetic field for sample values of the singlet-triplet scattering lengths: $a_s=-0.9R^*=-1873a_0$ and $a_t=-a_s$. Several broad magnetic resonances can be observed in the experimentally accessible range of magnetic fields. As for neutral atoms, such resonances can in principle be used in practice to tune the atom-ion effective interaction.

The MQDT results agree very well with the numerical results without higher-order dispersion terms, whereas one can observe very small discrepancies in the magnitude of a in comparison to the calculations performed with the full potential. Each resonance is associated with a bound molecular level crossing the energetically lowest atomic threshold, as shown in the lowest panel. The width of a resonance depends on particular molecular state crossing the threshold. For small interchannel coupling $1/a_c$ bound states occur mainly in a single asymptotic channel α, whereas for larger

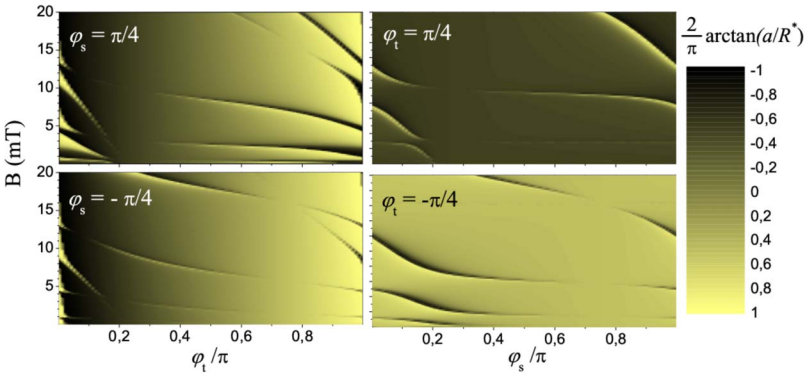

FIG. 3. (Color online) Contour plot of the dimensionless quantity $(2/\pi)\arctan(a/R^*)$ versus singlet and triplet short-range phases $\phi_s=-\arctan 1/a_s$ and $\phi_t=-\arctan 1/a_t$ and magnetic field B. In the leftmost panels, ϕ_s is fixed; in the rightmost panels, ϕ_t is fixed.

$1/a_c$ and weak magnetic fields, they are better characterized in terms of hyperfine angular momenta $\mathbf{F}$, f_1, and f_2.

The middle panel compares the radiative charge-transfer rate calculated numerically with the closed-coupling method and a local Einstein coefficient and MQDT with the semiclassical description of the short-range charge-transfer process. In the vicinity of resonances the charge-transfer rate is strongly enhanced as expected and the MQDT model seems to slightly overestimate it.

The range of magnetic fields in which the first Feshbach resonances should occur can be estimated from the energy location E^∞ of the associated bound states for $a=\infty$ and $B=0$. For a pure r^{-4} potential such energies are $E^\infty/E^*=105.8,1180,5208,\ldots$. Letting $\Delta\mu$ be the difference of magnetic moments between the Feshbach molecule and free atoms and assuming only a linear Zeeman shift for small values of B, we expect the first resonances to be found at $B<B_{\max}=E^\infty/\Delta\mu$, with $B_{\max}\,[\mathrm{mT}]=0.086,0.962,4.26$ for the Na-Ca^+ system.

In order to investigate the dependence of the position and strength of Feshbach resonances on the interatomic potentials, we show in Fig. 3 the variation of the quantity $2\arctan(a/R^*)/\pi$ with the singlet and triplet short-range phases $\phi_{s,t}=-\arctan 1/a_{s,t}$ and magnetic field B. Note that typically several resonances should be observable below $B\sim 20$ mT. One can remark that the resonances are usually relatively broad and only become very narrow when a_s and a_t are comparable and the interchannel coupling $1/a_c$ is small. Apart from the vicinity of resonances, the field-dependent scattering length is mainly determined by the value of a_t, which again is in turn related to the structure of the $\mathbf{Y}$ matrix.

In conclusion, a relatively simple quantum-defect model accurately describes atom-ion collisions in the ultracold domain, as verified by comparison with numerical coupled-channel calculations for the reference system $^{40}Ca^+$ and ^{23}Na. Our calculations predict that several magnetic Feshbach resonances should be available at relatively small values of magnetic fields to control the atom-ion interaction. Radiative charge exchange rates remain relative small even in the presence of Feshbach and shape resonances so that elastic collisions can be controlled without introducing unwanted losses.

We acknowledge support from the Office of Naval Research (P.S.J.), Polish Government research grant for years 2007–2010 (Z.I.), European Commission through the Integrated Project FET/QIPC "SCALA" (T.C.), and National Science Foundation through a grant for the Institute for Theoretical Atomic, Molecular and Optical Physics at Harvard University and Smithsonian Astrophysical Observatory (Z.I.,T.C.).

[1] A. T. Grier, M. Cetina, F. Oručević, and V. Vuletić, e-print arXiv:0808.3620.
[2] B. H. Bransden and M. R. C. McDowell, *Charge Exchange and the Theory of Ion-Atom Collisions* (Oxford University Press, Oxford, 1992).
[3] J. B. Delos, Rev. Mod. Phys. **53**, 287 (1981).
[4] M. J. Seaton, Rep. Prog. Phys. **46**, 167 (1983).
[5] Ch. H. Greene, A. R. P. Rau, and U. Fano, Phys. Rev. A **26**, 2441 (1982).
[6] F. H. Mies, J. Chem. Phys. **80**, 2514 (1984).
[7] M. J. Seaton and L. Steenman-Clark, J. Phys. B **10**, 2639 (1977); R. J. Drachman, *ibid.* **12**, L699 (1979).
[8] Apart from neutral-charged systems, the long-range r^{-4} potential describes effective interactions of polar molecules in a strong electric field: A. V. Avdeenkov and J. L. Bohn, Phys. Rev. A **66**, 052718 (2002).
[9] S. Watanabe and Ch. H. Greene, Phys. Rev. A **22**, 158 (1980).
[10] B. Gao, E. Tiesinga, C. J. Williams, and P. S. Julienne, Phys. Rev. A **72**, 042719 (2005).
[11] E. Vogt and G. H. Wannier, Phys. Rev. **95**, 1190 (1954).
[12] J. P. Burke, Jr., Ch. H. Greene, and J. L. Bohn, Phys. Rev. Lett. **81**, 3355 (1998).
[13] O. P. Makarov, R. Côté, H. Michels, and W. W. Smith, Phys. Rev. A **67**, 042705 (2003).
[14] B. Gao, Phys. Rev. A **64**, 010701(R) (2001).
[15] W. E. Milne, Phys. Rev. **35**, 863 (1930).
[16] R. M. Spector, J. Math. Phys. **5**, 1185 (1964).
[17] Z. Idziaszek, T. Calarco, and P. Zoller, Phys. Rev. A **76**, 033409 (2007).
[18] G. F. Gribakin and V. V. Flambaum, Phys. Rev. A **48**, 546 (1993).
[19] In the numerical calculation of elastic and charge-exchange rates, we neglect higher-order dipersion terms C_6 and C_8, which give rise to negligible corrections.
[20] P. S. Julienne and F. H. Mies, Phys. Rev. A **34**, 3792 (1986).
[21] P. S. Julienne, J. Chem. Phys. **68**, 32 (1978).